# A new discovery orichalcum ingots from Mediterranean sea: further investigation

Eugenio Caponetti[1,2], Francesco Armetta*[1], Lorenzo Brusca[4], Marco Ferrante[5], Delia Chillura Martino[1,2], Maria Luisa Saladino[1], Dario Guastella[6], Gabriella Chirco[6], Mario Berrettoni*[3], Silvia Zamponi[3], Paolo Conti[3] and Sebastiano Tusa[7]

[1]Dipartimento Scienze e Tecnologie Biologiche, Chimiche e Farmaceutiche – STEBICEF, Università degli Studi di Palermo, Parco d'Orleans II, Viale delle Scienze pad. 17, I-90128, Palermo, Italy
[2]Centro Grandi Apparecchiature-ATeN Center, Università degli Studi di Palermo, Via F.Marini 14, I-90128, Palermo, Italy
[3]Scuola di Scienze e Tecnologie sezione chimica, Università degli Studi di Camerino, Via S. Agostino 1, 62032 Camerino, Italy
[4]Istituto Nazionale di Geofisica e Vulcanologia – Sezione di Palermo, Via U. La Malfa 153, 90146, Palermo, Italy
[5] Trace Research Centre, Via I. Silone, 6, 64015, Nereto, Italy
[6]Labor Artis CR Diagnostica, Viale delle Scienze pad. 16, I-90128, Palermo, Italy
[7]Soprintendenza del mare della Regione Siciliana, Palazzetto Mirto Via Lungarini 9, I-90133 Palermo, Italy

*Corresponding author: francesco.armetta.ch@gmail.com and mario.berrettoni@unicam.it

## Abstract

In a recent time, 47 ingots were found in the seabed of Contrada Bulala (Gela) near the site where 40 ingots were previously recovered. The nature of the forty ingots, dated by the archaeologist in the VI century B.C., was determined as a Cu - Zn alloy known in that time as orichalcum.

The first question raised from an archaeological point of view, for the new discovery is whether the ingots of the first and the second excavations belonged to the same shipwreck.

Following the previous study an elementary analysis on the ingots of the second finding by using ICP-OS and ICP-MS techniques was performed. The chemometric treatment of the analytical results obtained on both sets, i.e. ingots from first and second discovery, confirms their similarity. Therefore, the two findings can be considered to belong to the same naval load. The lead isotopic ratios were determined on selected/representative ingots to improve the knowledge on this treasure. Results can provide information about probable location of the lead sources useful for the reconstruction of the trade routes in the Mediterranean Sea.

**KEYWORDS**: Orichalcum ingots, ICP-OES, ICP-MS, chemometric approach, Lead Isotopic ratio.

## 1   Introduction

The area of Bulala is located on the East side of the ancient Greek town of Gela (Sicily), on the left bank of the homonymous river that was flowing along the wide fertile plain that gave richness to the colony. The high number of archaeological objects recovered over time demonstrates the importance of Gela as an important trading center (Barone 2002). The intensive trading activities strongly affected the local economy with the development of local production as it is possible to observe for pottery factories whose local artisans started imitating products typical of Corinth, Rhodes and Crete but introduced new original styles (Panvini et al 1996). The ceramic production example is a strong evidence of the importance of this Greek colony on the trade in the Mediterranean area.

In front of this area the traces of an ancient wreck, carrying a precious load, was found; it was dated to the end of VI and beginning of V century B.C. In the same area in December 2014 the local diver Francesco Cassarino discovered 40 ingots of an alloy mainly constituted by copper and zinc. (Caponetti et al. 2017) this alloy, in ancient times was known as "orichalcum" and it was considered a precious metal, the third highest commercial value after gold and silver, nowadays this alloy is called brass. Following this important discovery, the Soprintendenza del Mare research team intensified the survey of the area by diving activities. Thank to those further surveys in February 2016 a new discovery of 47 ingots was made in the same area, few tens metres far from the first discovery.

The two findings strengthened a great interest from an historical and mythological point of view because Plato speaking about Atlantis used the word orichalcum. During the description of Atlantis, he wrote that this precious material was used for the decoration of the lost island (Lamb 1925). Furthermore, the discovery is more extraordinary due to the so large number of orichalcum ingots and their great amount (about 60 Kg).
A map for the localisation of the site of recovery and a picture of the ingots coming from the first and the second recovery are shown in figure 1.



*Figure 1 Location of site of recovery (A and B) and a photograph of ingots coming from the first and the second recovery (C).*

The ingots morphology is characteristic of mono-valve casting production, considering that each ingot has different sizes and that the shape is affected by several irregularities it is reasonable to think that they were subject of a handcraft production. The surface is clean and green corrosion products, typical of copper alloys buried in seawater, sometimes cover the yellowish metal.

The morphologic aspect and other archaeological evidence suggest that the ingots of the two discoveries are coeval, therefore, a batch of 83 ingots was studied; an administrative problem prevents us from investigating the other four ingots. They were characterized by (ICP-OS and ICP-MS) techniques that are commonly used for the study of ancient metal objects (Ponting et al. 1998, Botto et al. 2019). The analytical data were statistically treated by chemometric approaches (Li et al. 2015, Germundsson et al. 2015, Nemet et al. 2018) to reveal the degree of similarity and dissimilarities. The chemometric treatment (Massart et al. 1997, Massart

et al. 1998) of the obtained data divided the ingots in 5 clusters that could indicate different origin of the ingots, such as location of the furnace, type or provenience of the raw materials or other features. Some of us already published, in a previous paper, (Caponetti et al. 2017) the results obtained for the ingots of the first finding. The increased number of ingots, twice that of the first discovery (Caponetti et al. 2017), allowed us to perform a more reliable chemometric treatment of the data, and gave us the possibility to enhance the knowledge on this important finding of ancient metallic specimens. Taking into account that the amount of detected lead in several ingots suggests a voluntary addition to the alloy, the lead isotopic ratios on 24 ingots selected on the base of the five identified clusters were determined. These results allowed us to exclude the provenience of the lead from some regions and to formulate a hypothesis on its probable origin.

# 2   Materials and Methods

The ingots were weighted and measured to compare dimensions of the two sets. In a previous paper (Caponetti et al. 2017) some of us described the procedure of the quantitative elemental analysis on the ingots performed by coupling the ICP-OES for majority elements, and ICP-MS for trace elements. The use of both techniques is required due to the huge different amounts between major and trace elements. A multivariate data treatment procedure was used to draw some detailed information. Some ingots were previously analysed by using X-Ray Fluorescence Spectroscopy in order to evaluate the composition distribution, results indicated a high homogeneity for all the analysed spots of each ingot. This finding justifies our decision to perform one sampling for ingot, mainly, in order to reduce the invasive impact of the investigation.

The main elements of the alloy were determined by using an ICP-OES Jobin Yvon Ultima2 at wavelength of 324.754 nm for Cu and 213.856 nm for Zn (detection limits were 0.5 and 0.1 µg/L respectively). The amounts of trace elements were determined by ICP-MS Agilent 7500ce equipped with a Micromist nebulizer, a Scott double pass spray chamber, a three-channel peristaltic pump, an auto sampler (ASX-500, Cetac), and an octopole reaction system (ORS) to remove spectral interferences (detection limits in the order of 1 µg/L).

The set of samples described in reference **Errore. Il segnalibro non è definito.** is named A and each sample is coded by Sxx; the set of newly found samples is named B and each sample is coded by Mxx; xx is an increasing number. The use of the two codes is for sake of greater clarity in order to highlight the recovery set from which the sample originates. Despite the use of two different codes below, all the ingots were treated as a whole.

The simple analysis of the elemental composition is often not useful for drawing clear knowledge about some common features of the ingots, for this reason we performed a multivariate analysis to better investigate the hidden characteristics of the ingots.

All data were log10 transformed and then a robust scaling was applied. By using this data treatment (Vandeginste et al. 1998) major and trace element composition values get the same order of magnitude becoming comparable in term of absolute variability allowing us to minimize any influence due to concentration differences. That is, being $x_{i,j}$ the value measured on the $i^{th}$ sample (row of the datamatrix) for the $j^{th}$ element (column of the datamatrix) the robust standard deviation ($rSD_j$) estimate of column $j$ was calculated by using the following equation:

$$rSD_j = 1.4826 * median_j \left( \left| x_{i,j} - median_j \left( x_{i,j} \right) \right| \right) \ eq\ 1$$

From this, it can be obtained the robust autoscaling (Kurt at al. 2008) by substituting this formula in the formula of studentization of the variable (eq 2)

$$\widetilde{x}_{i,j} = \frac{x_{i,j} - median_j \left( x_{i,j} \right)}{1.4826 * median_j \left( \left| x_{i,j} - median_j \left( x_{i,j} \right) \right| \right)} \ eq\ 2$$

where $i$ varies from 1 to N (number of samples) and $j$ from 1 to the number of analyzed elements.

The isotopic determination was carried out by a TIMS MAT 262 VMC mass spectrometer from Finnigan (Bremen, D), located at the Laboratory of isotopic mass spectrometry (LIMS) of Laboratori Nazionali del Gran

Sasso (LNGS) Aquila - Italy. The instrument is equipped with 5 Faraday cups placed in a variable multi-collector, and with an extensive optical geometry. The software Spectromat, (Bremen, German) was used for data acquisition and analysis. Five blocks of ten replicates were acquired for each measurement in order to reach an associated average internal precision ≤30 ppm. Sample preparation was carried out in a ISO6 class clean room. Ultrapure nitric acid (DuoPUR, Milestone, Bergamo, Italia) and ultrapure 18.2 MΩ water from a Milli-Q (Millipore, USA) system were used for the sample treatment. SRM 981 isotopic standard from the National Standards and Technology (NIST Gaithersburg, MD, USA) was used for external precision measurement and method validation.

# 3   Results and discussion

## 3.1   Morphological aspects

From a visual investigation it is possible to recognize two main forms: a cigar-like and a flat bar-like. In both cases, the ingots are roughly refined indicating a rather primitive casting technique. The morphological aspect was studied by recording weight, length and width; the respective distributions are displayed in figure 2
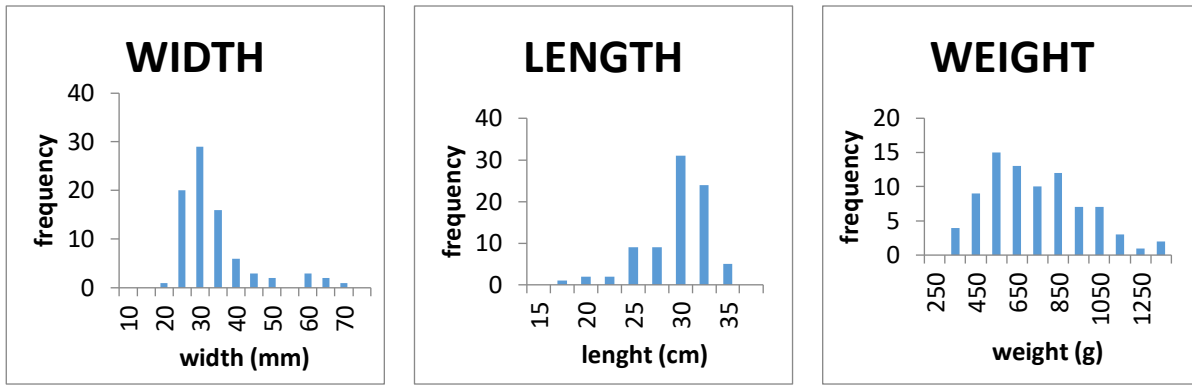
*Figure 2: Distribution of morphological indicators: weight, length and width.*

The distribution of length and width have a maximum at about 30 cm and 30 mm respectively with narrow ranges. In turns the weight histogram is spread over a wide interval ranging from 300 to 1000 g. The craftsmen seem to have paid attention in fixing a certain length and width. Probably the length was the main request from traders.

In any case, the technique probably used to make the mold directly by digging into the ground did not allow a great precision. The narrow distribution of length of the two sets may strengthen the hypothesis that all the ingots belong to the same load.

## 3.2    ICP Data analysis

The analytical results obtained from the ICP investigation performed on the samples, are reported in Table 1.

*Table 1: Elemental composition of the samples. Cu, Zn, Pb and Fe concentrations (%) and trace element concentrations (ppm) were determined by ICP-OES and by ICP–MS respectively.  (m=missing. Ti and Se were not analyzed in the first set of ingots while the same occur with Li for the second set)*

| Sample | Cu | Zn | Pb | Fe | Ni | Ag | Sb | As | Co | Cd | Sn | Te | Bi | Mn | Li | Al | V | Cr | Rb | Sr | Ba | Ti | Se |
|---|---|---|---|---|---|---|---|---|---|---|---|---|---|---|---|---|---|---|---|---|---|---|---|
| | % | % | % | % | ppm | ppm | ppm | ppm | ppm | ppm | ppm | ppm | ppm | ppm | ppm | ppm | ppm | ppm | ppm | ppm | ppm | ppm | ppm |
| S01 | 73 | 21 | 5.6 | 0.3 | 580 | 146 | 56 | 9.9 | 2.8 | 12.2 | 9.7 | 0.6 | 41.4 | 19.9 | 5.6 | 11.5 | 3.7 | 3.2 | 0.08 | 1.00 | 0.19 | m | m |
| S02 | 87 | 16 | 4.3 | 0.53 | 534 | 199 | 132 | 36.4 | 8.4 | 20.0 | 4.8 | 1.0 | 72.8 | 20.8 | 2.2 | 4.5 | 1.6 | 1.3 | 0.07 | 0.15 | 0.18 | m | m |
| S03 | 73 | 28 | 5.9 | 0.78 | 451 | 131 | 106 | 23.8 | 8.5 | 16.5 | 6.7 | 0.6 | 29.0 | 15.8 | 4.0 | 8.9 | 3.3 | 2.7 | 0.14 | 8.90 | 0.35 | m | m |
| S04 | 80 | 20 | 6.2 | 0.39 | 558 | 171 | 70 | 11.1 | 4.8 | 11.9 | 9.3 | 0.8 | 60.7 | 23.2 | 6.2 | 13.8 | 6.1 | 4.9 | 0.14 | 0.29 | 0.39 | m | m |
| S05 | 78 | 22 | 3.9 | 0.55 | 513 | 156 | 67 | 14.5 | 6.5 | 5.3 | 7.7 | 0.6 | 58.7 | 23.3 | 3.9 | 11.7 | 4.4 | 3.7 | 0.12 | 0.91 | 0.45 | m | m |
| S06 | 81 | 22 | 6.5 | 0.19 | 579 | 159 | 60 | 8.3 | 1.9 | 9.6 | 8.5 | 1.0 | 61.4 | 15.7 | 2.1 | 4.4 | 2.3 | 1.9 | 0.11 | 0.45 | 0.75 | m | m |
| S07 | 75 | 20 | 6.5 | 0.33 | 559 | 130 | 108 | 21.0 | 3.4 | 11.6 | 17.6 | 0.8 | 51.0 | 22.3 | 1.8 | 5.5 | 2.2 | 1.6 | 0.13 | 0.34 | 0.50 | m | m |
| S08 | 82 | 24 | 6.1 | 0.31 | 548 | 160 | 75 | 9.7 | 3.2 | 7.6 | 7.0 | 0.8 | 58.5 | 23.7 | 2.0 | 13.3 | 3.6 | 2.4 | 0.11 | 1.45 | 0.26 | m | m |
| S09 | 80 | 18 | 4.6 | 0.44 | 482 | 159 | 109 | 24.2 | 5.3 | 30.5 | 3.9 | 0.9 | 91.3 | 23.7 | 1.7 | 8.4 | 2.7 | 1.8 | 0.07 | 0.11 | 0.43 | m | m |
| S10 | 72 | 28 | 5.9 | 0.76 | 435 | 105 | 112 | 23.5 | 8.3 | 16.2 | 6.7 | 0.6 | 27.6 | 19.5 | 1.2 | 6.8 | 2.0 | 1.4 | 0.12 | 0.21 | 0.30 | m | m |
| S11 | 76 | 19 | 5.9 | 0.43 | 525 | 138 | 53 | 15.1 | 5.1 | 8.5 | 8.3 | 0.9 | 54.5 | 12.9 | 0.9 | 6.6 | 1.7 | 1.3 | 0.10 | 0.56 | 0.24 | m | m |
| S12 | 69 | 17 | 6.7 | 0.5 | 657 | 141 | 50 | 13.8 | 4.5 | 8.3 | 8.1 | 0.9 | 55.0 | 13.4 | 1.2 | 3.2 | 1.7 | 1.1 | 0.10 | 3.13 | 0.22 | m | m |
| S13 | 78 | 20 | 3.3 | 1.06 | 458 | 189 | 549 | 197.4 | 1.6 | 17.3 | 38.3 | 1.0 | 181.5 | 86.7 | 1.6 | 9.3 | 3.1 | 2.2 | 0.07 | 0.52 | 1.17 | m | m |
| S14 | 74 | 25 | 4.7 | 0.44 | 433 | 81 | 88 | 14.6 | 5.1 | 20.3 | 2.0 | 0.7 | 26.1 | 29.7 | 1.1 | 6.5 | 2.5 | 1.6 | 0.10 | 0.17 | 0.19 | m | m |
| S15 | 84 | 20 | 5.2 | 0.14 | 549 | 171 | 107 | 20.6 | 1.1 | 23.4 | 4.2 | 1.0 | 92.0 | 12.0 | 0.7 | 3.4 | 1.6 | 1.1 | 0.08 | 0.08 | 0.17 | m | m |
| S16 | 82 | 19 | 4.7 | 0.16 | 560 | 162 | 103 | 19.9 | 1.1 | 22.2 | 4.0 | 0.9 | 82.1 | 12.4 | 0.7 | 21.2 | 2.3 | 2.5 | 0.08 | 0.31 | 0.31 | m | m |
| S17 | 77 | 20 | 6.9 | 0.79 | 500 | 177 | 153 | 54.7 | 9.1 | 31.8 | 65.8 | 0.8 | 27.9 | 5.8 | 0.4 | 3.3 | 0.9 | 0.7 | 0.08 | 7.27 | 0.35 | m | m |
| S18 | 83 | 19 | 4.6 | 0.44 | 515 | 158 | 111 | 22.2 | 5.1 | 28.4 | 3.8 | 1.0 | 89.3 | 21.5 | 0.5 | 4.1 | 1.7 | 1.0 | 0.09 | 11.83 | 0.27 | m | m |
| S19 | 71 | 28 | 5.3 | 0.72 | 494 | 114 | 101 | 38.2 | 6.1 | 18.5 | 10.4 | 0.7 | 33.6 | 17.7 | 1.5 | 8.4 | 2.6 | 1.5 | 0.16 | 4.89 | 3.37 | m | m |

| | | | | | | | | | | | | | | | | | | | | | | | |
|---|---|---|---|---|---|---|---|---|---|---|---|---|---|---|---|---|---|---|---|---|---|---|---|
| S20 | 76 | 19 | 6.3 | 0.41 | 535 | 139 | 52 | 14.0 | 4.4 | 8.2 | 8.1 | 1.0 | 56.3 | 13.4 | 0.6 | 2.9 | 1.3 | 0.8 | 0.06 | 0.42 | 0.40 | m | m |
| S21 | 74 | 21 | 4.9 | 0.49 | 423 | 80 | 68 | 14.4 | 5.7 | 22.5 | 2.0 | 0.9 | 25.3 | 26.3 | 0.4 | 2.5 | 1.0 | 0.6 | 0.07 | 0.70 | 0.23 | m | m |
| S22 | 71 | 21 | 6.0 | 0.93 | 606 | 142 | 175 | 55.3 | 15.0 | 11.8 | 42.0 | 0.6 | 46.3 | 25.7 | 0.9 | 11.6 | 2.8 | 2.2 | 0.12 | 15.11 | 3.61 | m | m |
| S23 | 72 | 22 | 6.2 | 0.33 | 623 | 121 | 67 | 9.1 | 2.6 | 11.6 | 9.1 | 0.6 | 40.1 | 18.3 | 0.7 | 5.4 | 2.5 | 1.5 | 0.11 | 0.08 | 0.14 | m | m |
| S24 | 76 | 18 | 6.5 | 0.28 | 645 | 172 | 53 | 9.4 | 1.9 | 9.1 | 9.8 | 1.0 | 79.7 | 14.6 | 0.4 | 3.8 | 1.4 | 0.9 | 0.08 | 0.15 | 0.28 | m | m |
| S25 | 78 | 18 | 1.1 | 0.75 | 496 | 162 | 32 | 56.7 | 0.3 | 5.0 | 4.1 | 0.9 | 49.8 | 29.6 | 0.6 | 5.3 | 2.0 | 1.3 | 0.09 | 0.17 | 0.32 | m | m |
| S26 | 75 | 20 | 6.4 | 0.45 | 543 | 137 | 57 | 9.6 | 5.0 | 11.2 | 8.3 | 0.9 | 58.6 | 23.4 | 0.5 | 14.6 | 1.7 | 1.1 | 0.07 | 0.19 | 0.25 | m | m |
| S27 | 72 | 20 | 6.5 | 0.41 | 558 | 140 | 55 | 9.1 | 4.3 | 10.6 | 8.2 | 0.9 | 57.0 | 18.4 | 0.4 | 3.1 | 1.5 | 0.9 | 0.07 | 6.73 | 0.26 | m | m |
| S28 | 76 | 21 | 5.9 | 0.83 | 471 | 172 | 139 | 46.5 | 8.9 | 54.7 | 1.9 | 0.7 | 27.0 | 12.5 | 0.4 | 6.3 | 2.0 | 1.6 | 0.09 | 4.00 | 4.59 | m | m |
| S29 | 69 | 28 | 6.6 | 0.81 | 492 | 121 | 122 | 26.4 | 7.8 | 18.8 | 9.6 | 0.7 | 33.3 | 22.1 | 0.5 | 5.3 | 2.7 | 1.8 | 0.13 | 0.93 | 0.38 | m | m |
| S30 | 86 | 16 | 4.6 | 0.57 | 467 | 196 | 158 | 37.7 | 10.4 | 19.8 | 4.9 | 1.0 | 74.2 | 22.6 | 0.2 | 2.2 | 1.1 | 0.7 | 0.07 | 0.28 | 0.20 | m | m |
| S31 | 77 | 25 | 5.3 | 0.73 | 400 | 89 | 101 | 18.4 | 10.0 | 22.6 | 2.9 | 0.7 | 26.3 | 32.6 | 0.3 | 4.0 | 1.8 | 1.1 | 0.10 | 0.14 | 0.24 | m | m |
| S32 | 82 | 22 | 7.2 | 0.72 | 461 | 148 | 148 | 42.8 | 9.1 | 53.8 | 2.8 | 1.0 | 39.1 | 14.0 | 0.4 | 4.7 | 2.5 | 1.6 | 0.12 | 0.18 | 0.31 | m | m |
| S33 | 82 | 20 | 5.1 | 0.45 | 492 | 166 | 117 | 22.9 | 5.3 | 28.5 | 3.6 | 1.0 | 87.4 | 21.8 | 0.1 | 2.0 | 1.0 | 0.6 | 0.06 | 0.33 | 0.16 | m | m |
| S34 | 80 | 16 | 4.5 | 0.47 | 468 | 187 | 132 | 33.8 | 7.6 | 18.8 | 4.5 | 1.0 | 70.4 | 18.7 | 0.1 | 2.2 | 0.9 | 0.6 | 0.06 | 0.09 | 0.19 | m | m |
| S35 | 78 | 19 | 6.6 | 0.24 | 539 | 174 | 57 | 9.0 | 1.9 | 8.9 | 9.8 | 1.0 | 80.3 | 14.4 | 0.2 | 2.6 | 1.3 | 0.7 | 0.08 | 0.24 | 0.17 | m | m |
| S36 | 78 | 20 | 7.7 | 0.18 | 683 | 175 | 65 | 7.0 | 2.4 | 6.4 | 6.6 | 1.0 | 62.0 | 14.2 | 0.3 | 5.2 | 2.2 | 2.0 | 0.11 | 0.42 | 0.23 | m | m |
| S37 | 75 | 23 | 6.6 | 0.23 | 464 | 131 | 66 | 7.5 | 3.4 | 9.7 | 5.6 | 0.7 | 40.6 | 15.2 | 0.1 | 2.7 | 1.2 | 1.0 | 0.09 | 2.88 | 0.12 | m | m |
| S38 | 90 | 21 | 2.3 | 0.38 | 656 | 165 | 125 | 201.0 | 0.9 | 24.8 | 15.7 | 1.8 | 150.6 | 79.1 | 0.4 | 9.0 | 4.0 | 2.3 | 0.22 | 2.20 | 0.42 | m | m |
| M01 | 76 | 21 | 3.5 | 0.53 | 398 | 120 | 58 | 14.3 | 7.2 | 5.0 | 5.4 | 0.9 | 50.4 | 22.2 | m | 10.2 | 0.25 | 0.38 | 0.10 | 0.44 | 0.18 | 0.67 | 0.39 |
| M02 | 70 | 21 | 5.9 | 0.28 | 455 | 129 | 66 | 8.8 | 3.1 | 7.0 | 4.8 | 1.3 | 52.8 | 26.0 | m | 92.3 | 0.32 | 0.34 | 0.20 | 1.64 | 0.46 | 2.60 | 0.59 |
| M03 | 78 | 18 | 4.1 | 0.13 | 440 | 135 | 97 | 20.9 | 1.2 | 22.9 | 3.0 | 1.4 | 76.2 | 12.8 | m | 9.6 | 0.03 | 0.21 | 0.07 | 0.86 | 0.08 | 0.52 | 0.49 |
| M04 | 76 | 14 | 3.5 | 0.45 | 422 | 154 | 126 | 35.2 | 8.4 | 19.4 | 3.4 | 1.4 | 63.9 | 20.4 | m | 2.8 | 0.01 | 0.14 | 0.08 | 0.04 | 0.12 | 0.32 | 0.57 |
| M05 | 73 | 21 | 5.7 | 0.17 | 425 | 115 | 50 | 7.7 | 2.3 | 7.7 | 10.5 | 1.3 | 46.9 | 20.2 | m | 8.8 | 0.02 | 0.12 | 0.08 | 0.32 | 0.05 | 0.35 | 0.45 |
| M06 | 73 | 20 | 5.4 | 0.26 | 448 | 128 | 64 | 8.5 | 3.0 | 7.8 | 4.5 | 1.4 | 52.4 | 22.2 | m | 5.7 | 0.02 | 0.14 | 0.08 | 0.87 | 0.03 | 0.40 | 0.49 |
| M07 | 72 | 22 | 4.3 | 1.35 | 482 | 129 | 188 | 73.9 | 17.8 | 11.3 | 23.8 | 1.2 | 56.1 | 13.6 | m | 6.7 | 0.03 | 0.19 | 0.09 | 1.45 | 0.23 | 0.40 | 0.64 |
| M08 | 78 | 17 | 4.2 | 0.13 | 426 | 143 | 103 | 22.1 | 1.2 | 23.8 | 3.1 | 1.4 | 76.7 | 13.1 | m | 8.6 | 0.01 | 0.14 | 0.09 | 0.08 | 0.17 | 0.52 | 0.66 |
| M09 | 81 | 15 | 3.7 | 0.49 | 438 | 166 | 135 | 38.4 | 9.0 | 20.8 | 3.8 | 1.4 | 65.8 | 21.1 | m | 5.9 | 0.01 | 0.07 | 0.08 | 0.37 | 0.10 | 0.40 | 0.63 |
| M10 | 77 | 18 | 4.2 | 0.47 | 399 | 195 | 139 | 56.2 | 6.3 | 23.3 | 15.3 | 1.4 | 32.1 | 8.8 | m | 3.7 | 0.07 | 0.15 | 0.08 | 0.12 | 0.13 | 0.35 | 0.52 |
| M11 | 78 | 18 | 4.1 | 0.4 | 422 | 128 | 109 | 24.5 | 5.6 | 30.0 | 2.8 | 1.4 | 80.6 | 22.5 | m | 1.0 | 0.01 | 0.14 | 0.08 | 0.04 | 0.18 | 0.20 | 0.55 |
| M12 | 75 | 20 | 5.6 | 0.18 | 474 | 128 | 59 | 7.9 | 1.8 | 9.0 | 5.8 | 1.4 | 49.7 | 16.1 | m | 10.3 | 0.01 | 0.10 | 0.08 | 0.02 | 0.03 | 0.55 | 0.60 |
| M13 | 78 | 18 | 3.9 | 0.69 | 490 | 96 | 121 | 59.8 | 10.3 | 16.6 | 11.0 | 1.3 | 51.8 | 11.6 | m | 6.9 | 0.08 | 0.37 | 0.10 | 4.03 | 0.32 | 0.60 | 0.68 |
| M14 | 62 | 28 | 5.7 | 0.7 | 375 | 101 | 118 | 30.5 | 7.9 | 13.9 | 6.8 | 1.1 | 29.7 | 30.7 | m | 9.3 | 0.11 | 0.90 | 0.06 | 1.19 | 0.15 | 0.49 | 0.61 |
| M15 | 71 | 18 | 5.5 | 0.42 | 502 | 133 | 57 | 10.9 | 4.3 | 7.8 | 6.5 | 1.3 | 55.8 | 22.6 | m | 1.0 | 0.04 | 0.07 | 0.04 | 0.08 | 0.08 | 0.16 | 0.53 |
| M16 | 68 | 21 | 5.2 | 0.27 | 477 | 129 | 66 | 8.8 | 3.0 | 7.6 | 4.5 | 1.3 | 46.0 | 21.7 | m | 1.9 | 0.02 | 0.09 | 0.05 | 0.06 | 0.29 | 0.30 | 0.47 |
| M17 | 77 | 17 | 4.0 | 0.43 | 450 | 139 | 112 | 26.3 | 6.0 | 30.1 | 2.7 | 1.3 | 79.4 | 26.3 | m | 2.5 | 0.07 | 0.17 | 0.06 | 0.04 | 0.15 | 0.41 | 0.58 |
| M18 | 68 | 25 | 5.6 | 0.71 | 375 | 94 | 116 | 27.2 | 8.8 | 18.1 | 5.0 | 1.0 | 25.2 | 19.0 | m | 9.6 | 0.07 | 0.24 | 0.06 | 0.10 | 0.08 | 0.46 | 0.55 |
| M19 | 76 | 17 | 3.9 | 0.43 | 448 | 135 | 109 | 24.7 | 5.9 | 29.4 | 2.7 | 1.3 | 75.3 | 18.9 | m | 1.0 | 0.03 | 0.97 | 0.06 | 6.46 | 0.92 | 0.34 | 0.46 |
| M20 | 79 | 15 | 3.8 | 0.52 | 453 | 167 | 146 | 40.3 | 11.2 | 22.7 | 3.9 | 1.4 | 67.9 | 27.1 | m | 5.1 | 0.04 | 0.13 | 0.08 | 0.31 | 0.21 | 0.60 | 0.56 |
| M21 | 78 | 20 | 0.9 | 1.37 | 442 | 191 | 89 | 190.2 | 0.8 | 5.8 | 10.5 | 1.3 | 49.3 | 34.1 | m | 4.1 | 0.06 | 0.15 | 0.09 | 0.27 | 0.08 | 0.29 | 0.84 |
| M22 | 75 | 16 | 4.1 | 0.45 | 429 | 142 | 116 | 26.5 | 6.0 | 29.8 | 2.8 | 1.3 | 75.6 | 25.2 | m | 8.4 | 0.09 | 0.12 | 0.09 | 0.28 | 0.13 | 0.45 | 0.64 |
| M23 | 73 | 17 | 4.5 | 0.5 | 444 | 205 | 142 | 58.3 | 6.6 | 24.1 | 16.2 | 1.2 | 31.3 | 9.5 | m | 10.9 | 0.04 | 0.16 | 0.07 | 0.11 | 0.08 | 0.37 | 0.44 |
| M24 | 74 | 16 | 5.7 | 0.84 | 518 | 213 | 199 | 65.3 | 12.2 | 28.0 | 15.9 | 1.1 | 41.8 | 12.6 | m | 6.0 | 0.05 | 0.13 | 0.09 | 1.76 | 0.21 | 0.40 | 0.59 |
| M25 | 69 | 23 | 6.8 | 1.39 | 398 | 228 | 173 | 92.2 | 19.2 | 77.7 | 16.7 | 1.0 | 31.9 | 8.6 | m | 1.0 | 0.06 | 0.14 | 0.08 | 0.01 | 0.25 | 0.21 | 0.87 |
| M26 | 75 | 16 | 4.5 | 0.47 | 464 | 145 | 119 | 27.8 | 6.1 | 30.8 | 2.9 | 1.3 | 80.2 | 26.2 | m | 1.0 | 0.17 | 0.10 | 0.08 | 0.52 | 0.14 | 0.23 | 0.69 |
| M27 | 75 | 16 | 4.5 | 0.47 | 480 | 146 | 120 | 26.8 | 6.2 | 31.0 | 2.8 | 1.3 | 80.2 | 26.5 | m | 1.1 | 0.08 | 0.07 | 0.06 | 0.70 | 0.08 | 0.26 | 0.59 |

| | | | | | | | | | | | | | | | | | | | | | | | |
|---|---|---|---|---|---|---|---|---|---|---|---|---|---|---|---|---|---|---|---|---|---|---|---|
| M28 | 74 | 15 | 3.8 | 0.34 | 426 | 209 | 111 | 39.7 | 4.5 | 12.2 | 10.2 | 1.1 | 32.1 | 54.1 | m | 79.5 | 0.53 | 0.53 | 0.17 | 21.16 | 1.65 | 2.87 | 0.38 |
| M29 | 71 | 17 | 6.4 | 0.43 | 488 | 129 | 61 | 11.3 | 5.8 | 12.0 | 6.5 | 1.2 | 51.0 | 24.7 | m | 17.6 | 0.14 | 0.14 | 0.09 | 2.24 | 0.23 | 1.94 | 0.63 |
| M30 | 65 | 23 | 5.7 | 0.77 | 405 | 96 | 111 | 27.5 | 8.9 | 18.7 | 7.2 | 1.1 | 30.8 | 25.0 | m | 6.2 | 0.11 | 0.15 | 0.12 | 0.33 | 0.17 | 0.58 | 0.86 |
| M31 | 73 | 16 | 4.0 | 0.49 | 472 | 141 | 111 | 25.0 | 6.2 | 28.3 | 2.6 | 1.2 | 71.0 | 18.7 | m | 13.3 | 0.29 | 0.32 | 0.09 | 7.84 | 0.61 | 0.96 | 0.54 |
| M32 | 65 | 21 | 7.0 | 1.55 | 534 | 163 | 314 | 139.1 | 38.4 | 7.4 | 25.3 | 0.8 | 42.2 | 12.3 | m | 6.7 | 0.14 | 0.21 | 0.10 | 0.74 | 0.30 | 0.59 | 0.51 |
| M33 | 73 | 16 | 4.9 | 0.14 | 462 | 149 | 106 | 24.3 | 1.4 | 25.6 | 3.4 | 1.4 | 79.7 | 15.8 | m | 12.7 | 0.17 | 0.18 | 0.10 | 19.97 | 0.25 | 0.62 | 0.65 |
| M34 | 77 | 14 | 4.2 | 0.57 | 490 | 172 | 149 | 41.2 | 10.8 | 21.8 | 3.9 | 1.3 | 63.9 | 25.9 | m | 3.6 | 0.03 | 0.12 | 0.09 | 0.48 | 0.18 | 0.42 | 0.62 |
| M35 | 70 | 19 | 5.7 | 0.68 | 485 | 117 | 61 | 13.1 | 7.6 | 10.6 | 5.7 | 1.0 | 40.0 | 30.7 | m | 1.0 | 0.01 | 0.13 | 0.06 | 0.03 | 0.07 | 0.16 | 0.58 |
| M36 | 75 | 16 | 4.2 | 0.56 | 507 | 176 | 146 | 40.0 | 9.9 | 21.0 | 3.7 | 1.2 | 61.0 | 23.7 | m | 8.8 | 0.01 | 0.06 | 0.07 | 0.72 | 1.87 | 0.40 | 0.56 |
| M37 | 75 | 16 | 4.7 | 0.15 | 487 | 154 | 110 | 24.2 | 1.2 | 23.5 | 3.2 | 1.2 | 75.0 | 14.0 | m | 1.0 | 0.08 | 0.10 | 0.07 | 0.09 | 0.10 | 0.10 | 0.54 |
| M38 | 71 | 19 | 4.9 | 0.44 | 462 | 150 | 54 | 12.9 | 5.9 | 10.1 | 4.1 | 1.1 | 64.8 | 19.4 | m | 14.9 | 0.03 | 0.06 | 0.06 | 0.05 | 0.54 | 0.45 | 0.30 |
| M41 | 69 | 21 | 3.9 | 0.58 | 436 | 129 | 63 | 15.3 | 7.3 | 5.1 | 5.3 | 0.9 | 46.7 | 25.9 | m | 1.0 | 0.09 | 0.11 | 0.03 | 0.44 | 0.07 | 0.18 | 0.32 |
| M42 | 73 | 18 | 4.7 | 0.14 | 462 | 145 | 103 | 23.8 | 1.2 | 24.0 | 3.1 | 1.2 | 72.9 | 14.0 | m | 1.0 | 0.14 | 0.14 | 0.03 | 0.03 | 0.05 | 0.15 | 0.64 |
| M43 | 74 | 16 | 5.0 | 0.13 | 466 | 152 | 105 | 24.7 | 1.2 | 24.9 | 3.3 | 1.3 | 74.9 | 14.2 | m | 1.0 | 0.09 | 0.15 | 0.03 | 0.07 | 0.07 | 0.10 | 0.70 |
| M44 | 75 | 16 | 4.5 | 0.43 | 450 | 139 | 107 | 27.1 | 6.1 | 30.5 | 2.8 | 1.2 | 78.4 | 24.5 | m | 5.5 | 0.08 | 0.10 | 0.03 | 0.07 | 0.06 | 0.30 | 0.62 |
| M45 | 72 | 18 | 3.5 | 0.85 | 490 | 199 | 113 | 27.8 | 9.9 | 8.8 | 15.9 | 0.9 | 98.9 | 14.9 | m | 1.0 | 0.03 | 0.09 | 0.05 | 0.58 | 1.31 | 0.25 | 0.57 |
| M46 | 72 | 17 | 5.7 | 0.37 | 490 | 126 | 59 | 10.2 | 4.7 | 5.3 | 5.4 | 1.2 | 46.6 | 20.4 | m | 3.3 | 0.10 | 0.10 | 0.04 | 0.14 | 0.03 | 0.32 | 0.55 |
| M47 | 65 | 24 | 5.4 | 0.73 | 415 | 93 | 104 | 28.5 | 8.6 | 17.3 | 6.8 | 1.0 | 27.3 | 23.6 | m | 2.5 | 0.10 | 0.09 | 0.04 | 0.03 | 0.04 | 0.46 | 0.78 |

The error is one unity on the last digit.

Because of the large difference between element concentration, data were transformed as $x = \log_{10}(x)$. After this transformation, all the statistical parameters such as quartiles, intervals, means and outliers for all the ingots are reported in a synoptic way in figure**Errore. L'origine riferimento non è stata trovata.**S1 of support information. The main elements are copper and zinc. It is important to point out that the zinc amount varying from 15.11 to 28.46 % in weight, is compatible with the preparation of the alloy obtained by means of the cementation process (Bourgarit et al. 2010).

Lead is a minor element with a concentration comprised in the range 0.80 - 7.71 % indicating that it was intentionally added, at least in the ingots with higher content. It is well known that lead is not soluble in copper lattice, unlike zinc, and tends to segregate in dispersed domains, so even if it improves the fluidity of the molten alloy, the resulting solid metal has poor mechanical properties (Ingo et al. 2019). That considered, it is possible to suppose that the ingots were prepared with the idea to use the alloy for melting processes instead of handwork ones. Iron content is comprised in the range 0.13-1.55%. Nickel and silver are present with hundreds of ppm, while Sb, As, Co, Cd, Sn, Te, Bi, Mn, Li, Al, V, Cr, Rb, Sr, Ba, Ti and Se are lower than 100 ppm.

### 3.3 Multivariate analysis

#### 3.3.1 Cluster Analysis

As the knowledge about these ingots is very poor, we tried, at first, a cluster analysis by Ward's methods that would permit us to hypothesize some cluster that could be associated to some hidden characteristics. The results of the cluster analysis are shown in figure .
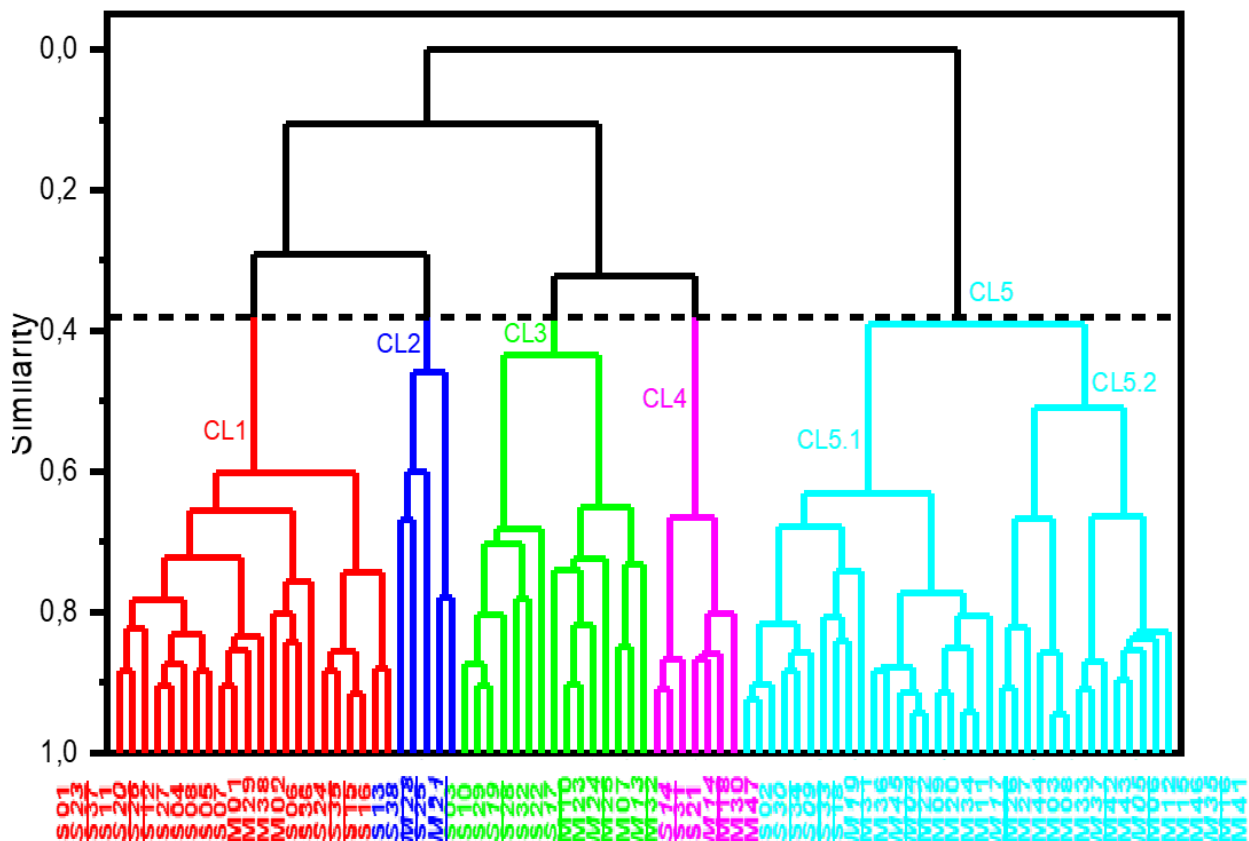
*Figure 3: Ward's cluster of robust scaled data. Italic underlined abscissa labels indicate those samples for which the Pb isotopic ratios were determined.*

The dendrogram shows a hierarchy of clusters that come together at different levels of similarity. There is no effective criterion for determining how many clusters reflect the true intrinsic characteristics of the objects under investigation. A good rule of thumb is to seek a comparison with external knowledge that allows confirmation of the partitioning. Here we have no such external knowledge, but it is possible to verify the results obtained from clustering if we use them as input for multivariate methods of classification (Massart et al. 1998). By considering a threshold similarity a bit greater than 0.38 (a value highlighted by the black dotted line in the figure) the entire set of ingots is divided into five subsets that will be used as the input class of the classification methods. Hereafter we indicate the resulting clusters by CLx where x stands for an increasing number.

In table 2 we report the composition and population of each cluster.

The colors correspond to the ones used to identify the clusters in figure  while the colors of the underlines highlight the clusters in **Errore. L'origine riferimento non è stata trovata.**: Black, Red, Blue and Magenta indicate cluster 1, 2, 3 and 4 respectively.

*Table 2: Clusters population*

| Cluster | Ingot | _Tot |
|---|---|---|
| CL1 | S01, S04, S05, S06, S07, S08, S11, S12, S15, S16, S20, S23, S24, S26, S27, S35, S36, S37, M01, M02, M29, M38 | 22 |
| CL2 | S13, S25, S38, M21, M28 | 5 |
| CL3 | S03, S10, S17, S19, S22, S28, S29, S32, M07, M10, M13, M23, M24, M25, M32 | 15 |
| CL4 | S14, S21, S31, M14, M18, M30, M47 | 7 |

| CL5 | S02, S09, S18, S30, S33, S34, M04, M09, M11, M17, M19, M20, M22, M26, M27, M31, M34, M36, M44, M45, M03, M05, M06, M08, M12, M15, M16, M33, M35, M37, M41, M42, M43, M46 | 34 |
|------|------|------|

A more detailed analysis shows that:

- the classification highlights three mains clusters: CL1, CL3 and CL5, that represent the 86% of the population;
- there are two less populated clusters, CL2 and CL4, that can be considered relatives of CL1 and CL3 respectively;
- the cluster CL5 could be divided in two cluster CL5.1 and CL5.2 fixing a little bit higher value for the similarity threshold. In that case the cluster CL5.2 would group only samples of the second discovery;
- the simultaneous presence of ingots Mxx and Sxx in the clusters is strong evidence of similarity of the ingots of the two discoveries, therefore it is possible to confirm the archaeologist's hypothesis about the origin of the ingots from the same wreck.

The PCA analysis, reported in support information (Figure S2) confirms the clustering results of the WARD's diagram.

### 3.3.2    Classification

We attempt a check of the clusters above described executing Linear Discriminant Analysis (LDA) in the hypothesis that the groups defined with 5 clusters are due to actual features; clusters were used as the classification characteristic. CL2 was excluded by the analysis because the number of samples in it is much lower than in any other of the clusters, **Errore. L'origine riferimento non è stata trovata.** of support information reports the obtained results. We applied LDA on the principal component scores retaining only six of them. The analysis confirms the four clusters with total classification ability of 97.0% and a 96.1% prediction ability estimated by leave-one-out cross-validation. A further check of the obtained results was done by the non-parametric modeling method SIMCA that as compared to LDA is more robust against outliers (Table SII of support information). The results of the two methods are comparable.

Both trials largely confirm the results obtained by clustering the samples. An indication of the most important elements characterizing the clusters is given by the discriminant power computed by SIMCA (Table SIII of support information).

As looking at figure  it is possible to hypothesize two subclusters (CL5.1 and CL5.2) of CL5 hence we verified by classification (data not shown) even the existence of six clusters. The results obtained, also in this case CL2 was not considered for the previously asserted reason, is similar to that with 5 clusters. Subclusters CL5.1 and CL5.2 could exist, in this case it would be present a further group (CL5.2) including only samples of the second finding. The drastic increment of the population in the statistical analysis performed permits results with a higher degree of confidence and, consequently, more reliable conclusions in comparison whit our previous results (Caponetti et al.2017).

The confirmed existence of different clusters suggests both a different way of manufacturing, different furnaces and, possibly, a different origin of raw materials.

## 3.4    Pb isotopic ratio

As previously considered, in several ingots the lead was intentionally added. The driving force of the grouping ability can be the provenance of the raw material for their production. Among the method to disclose the provenance of some metals there is the isotopic ratio analysis that is particularly developed and utilized (Gale 2009, Zhengfeng et al. 2016, Liu et al. 2018) for the lead.

It is known that the lead isotopic ratio analysis is the most powerful method for provenance attribution of this metal even if it should be emphasized that the origin of the lead can be distorted by the casting technique, for example with a partial recasting of older artifacts (Pollard et al 2008).

On the base of these considerations, we have performed the analysis of the isotopic ratio on 24 ingots chosen as representative of the 5 clusters. The obtained results are reported in Table 3.

*Table 3: Lead isotopic ratios of the analyzed samples (error is a unity of the last digit)*

| Sample | 206Pb/204Pb | 208Pb/206Pb | 207Pb/206Pb |
|--------|-------------|-------------|-------------|
| S17 | 18.3248 | 2.09920 | 0.85446 |
| M14 | 18.3359 | 2.09874 | 0.85400 |
| S19 | 18.3421 | 2.09845 | 0.85373 |
| M45 | 18.3694 | 2.09775 | 0.85269 |
| M17 | 18.3696 | 2.09760 | 0.85263 |
| S33 | 18.3707 | 2.09761 | 0.85262 |
| S09 | 18.3705 | 2.09762 | 0.85262 |
| M19 | 18.3705 | 2.09757 | 0.85260 |
| M35 | 18.3735 | 2.09748 | 0.85248 |
| M37 | 18.3736 | 2.09745 | 0.85248 |
| S23 | 18.3783 | 2.09739 | 0.85228 |
| S30 | 18.3984 | 2.09654 | 0.85148 |
| M04 | 18.3988 | 2.09654 | 0.85147 |
| S14 | 18.3991 | 2.09650 | 0.85138 |
| S26 | 18.4038 | 2.09647 | 0.85126 |
| M05 | 18.4088 | 2.09624 | 0.85104 |
| S20 | 18.4089 | 2.09623 | 0.85101 |
| M24 | 18.4127 | 2.09586 | 0.85087 |
| M28 | 18.4167 | 2.09560 | 0.85069 |
| M13 | 18.4222 | 2.09577 | 0.85050 |
| S35 | 18.4252 | 2.09566 | 0.85037 |
| S24 | 18.4267 | 2.09563 | 0.85032 |
| M21 | 18.5609 | 2.08922 | 0.84466 |
| S38 | 18.5649 | 2.08784 | 0.84443 |

The lead isotopic ratios of Oxalid database together with the ones of our samples are reported in figure 4.
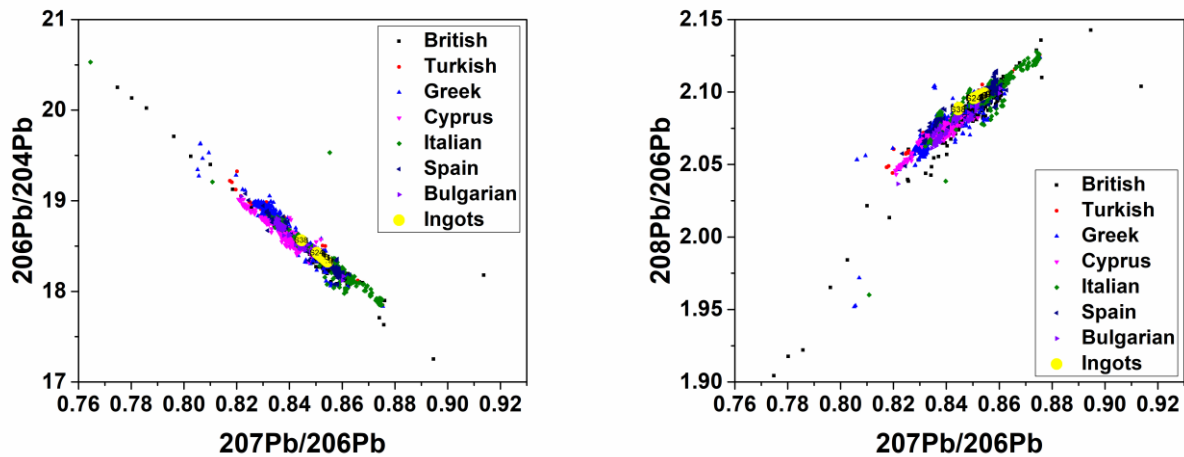
*Figure 4: Graphic representation of Lead isotopic ratios of our samples together with the ones of Oxalid database.*

As observed in figure 4 the isotopic ratio values of our samples gather in small regions of the graphic representation. The magnifications of these regions are reported in figure 5.
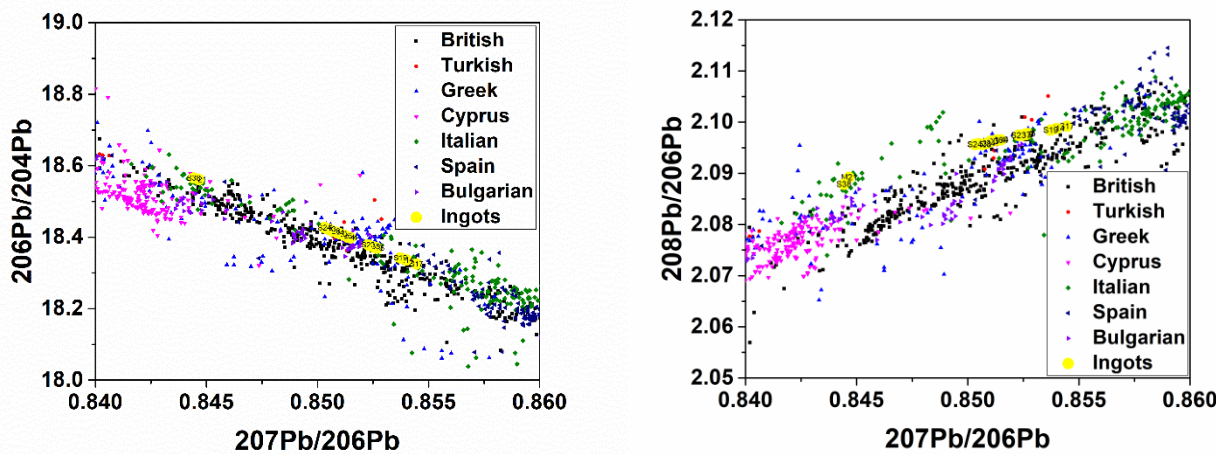


*Figure 5: Magnifications of the regions highlighted in fig. 4*

Even if the isotopic ratios of our samples have close values, they can be assembled in four groups. Each group is constituted by ingots coming from the two discoveries. These groups are in four regions of the lead isotopic ratios graphic representation where there are some spots of Oxalid database from different geographical areas. These finding exclude the lead provenience from some regions such as Turkey, Great Britain and Bulgaria, but prevents the possibility of a precise geographic identification. Despite of that, the hypothesis that Greece, Italy and Spain are the most probable locations of the lead sources can be made.

The above considerations are in agreement with the conclusion derived from ICP results joint to the statistical treatment and allow us to state that the 83 analyzed orichalcum ingots of the two findings can be considered to belong to the same naval load, and that they originate from different geographic regions. These finding can be also useful for the reconstruction of the trade routes in the Mediterranean Sea.

# 4 Conclusion

The new set of orichalcum ingots discovered in the Bulala area (Gela-Sicily) in February 2016 gave us the opportunity to investigate a number of samples that is twice the one related to the recovery in December 2014; this makes the results of the work more coherent and harbingers of new perspectives.

The entire amount of orichalcum recovered in the two discoveries is more than 60 Kg, a huge quantity in comparison to the few and small brass artifacts displayed or collected in the museums of the Mediterranean area.

The PCA and cluster analysis of ICP chemical composition data, divide the whole number of ingots in five clusters each including ingots belonging to the two sets. The existence of these clusters is an interesting result for the archaeological as well as historical interpretation of this important discovery. The three main clusters, CL1, CL3, and CL5, represent the 87% of the total number of ingots. This issue confirms that the two sets of ingots belong to the same naval load.

The clusters identified by the clustering procedure were the starting point for a more expensive and time-consuming analysis such as the determination of Lead isotopic ratios. In fact, results of cluster analysis allowed us to perform a well thought out selection of some representative ingots providing the possibility of reducing the number of ingots to be analyzed. The selection allowed us to run the lead isotopic ratios analysis that would otherwise be precluded for all the ingots.

The results of the Lead isotopic ratio analysis confirmed the belonging of the two sets of ingots to the same load and assigned the most probable origin of the Lead to Greece, Italy and Spain.

Even if we can, only predict from a probabilistic point of view the geographical origins of the lead added to the Copper - Zinc alloy, the obtained results allowed us to exclude others suitable regions as origin of the lead. The classification results and the hypothesis on the lead origin are useful data to pursue a deeper study on the orichalcum trade in the Mediterranean area.

## 4.1    Acknowledgements

**Figure Caption**

Figure 1 Location of site of recovery (A and B) and a photograph of ingots coming from the first and the second recovery (C).

Figure 2: Distribution of morphological indicators: weight, length and width.

Figure 3: Ward's cluster of robust scaled data. Italic underlined abscissa labels indicate those samples for which the Pb isotopic ratios were determined.

Figure 4: Graphic representation of Lead isotopic ratios of our samples together with the ones of Oxalid database.

Figure 5: Magnifications of the regions highlighted in fig. 4

References

Barone G., 2002, Preliminary archaeometric analysis on amphorae, in VI and V centuries B.C., from excavations at Gela (Sicily), Per. Mineral., 71, 3, 273-287.

Botto, A., Campanella, B., Legnaioli, S., Lezzerini, M., Lorenzetti, G., Pagnotta, S., Poggialini, F. and Palleschi, V., 2019, Applications of laser-induced breakdown spectroscopy in cultural heritage and archaeology: a critical review, J. Anal. At. Spectrom., 34, 81-103, DOI: 10.1039/C8JA00319J.

Bourgarit D., Bauchau F., 2010, The ancient brass cementation processes revisited by extensive experimental simulation, Feature Archaeotechnology, 62, 3, 27–33, DOI: 10.1007/s11837-010-0045-3.

Caponetti, E., Armetta, F., Brusca, L., Chillura Martino, D., Saladino, M.L., Ridolfi, S., Chirco, G., Berrettoni, M., Conti, P., Nicolò, B. and Tusa, S., 2017, A multivariate approach to the study of orichalcum ingots from the underwater Gela's archaeological site, Microchemical Journal, 135, 163–170, DOI: 10.1016/j.microc.2017.09.003.

Caponetti, E., Armetta, F., Chillura Martino, D., Saladino, M.L., Ridolfi, S., Chirco, G., Berrettoni, M., Conti, P., Nicolò, B. and Tusa, S., 2017, First discovery of orichalcum ingots from the remains of a 6th century BC shipwreck near Gela (Sicily) seabed, Mediterranean Archaeology and Archaeometry, 17(2), 11-18, DOI: 10.5281/zenodo.581716.

Stos-Gale, Z.A. and Gale, N.H., 2009, Metal provenancing using isotopes and the Oxford archaeological lead isotope database (OXALID) Archaeol Anthropol Sci, 1, 195-213, DOI 10.1007/s12520-009-0011-6.

Germundsson, B., Pihl, A. and Esbensen, K. H., 2015, Proper sampling for archeometric discrimination of Bronze-age fields on Bornholm, Denmark – Archaeology meets TOS meets Chemometrics, TOS forum 5, 199-203, DOI: 10.1255/tosf.67.Kurt, V. and Filzmoser, P., 2008, Introduction to Multivariate Statistical Analysis in Chemometrics, Taylor & Francis: Boca Raton, ISBN 978-1-4200-5947-2.

Ingo G.M., Riccuccia, C., Guida, G., Pascucci, M., Giuliani, C., Messina, E., Fierro, G., Di Carlo, G., 2019, Micro-chemical investigation of corrosion products naturally grown on archaeological Cu-based artefacts retrieved from the Mediterranean sea, Applied Surface Science 470, 695–706.

Li, P., Cai, W. and Shao, X., 2015, Improved inductively coupled plasma optical emission spectroscopy analysis of trace elements in complex matrices by chemometric resolution, J. Anal. At. Spectrom. 30, 936-940, DOI: 10.1039/C5JA00031A.

Liu, R., Rawson, J. and Pollard. A. M., 2018, Beyond ritual bronzes: identifying multiple sources of highly radiogenic lead across Chinese history, Scientific Reports 8, 11770, DOI: 10.1038/s41598-018-30275-2.

Massart, D. L., Vandeginste, B. G. M., Buydens, L. M. C., De Jong, S., Lewi, P. J., and Smeyers-Verbeke, J., 1997, Handbook of Chemometrics and Qualimetrics: Part A in Data Handling in Science and Technology Volume 20A, Elsevier: Amsterdam, Xvii + 867. ISBN 0-444-89724-0.

Massart, D. L., Vandeginste, B. G. M., Buydens, L. M. C., De Jong, S., Lewi, P. J., and Smeyers-Verbeke, J., 1998, Handbook of Chemometrics and Qualimetrics: Part B" in "Data Handling in Science and Technology Volume 20B, Elsevier: Amsterdam, 732. ISBN 0-444-82853-2.

Nemet, I., Rončević, S., Bugar, Al., Ferri, T. Z., and Pitarević, L., 2018, Classification analysis of archaeological findings from early-iron production (Turopolje region, NW Croatia) based on multi-analytical profiling, J. Anal. At. Spectrom. 33, 2053-2061, DOI: 10.1039/C8JA00202A.

Lamb, W.R.M.., 1925, Plato in Twelve Volumes, Vol. 9 translated by Cambridge, MA, Harvard University Press; London, William Heinemann Ltd.

Pollard, A.M., Heron, C., 2008, Archaeological chemistry, 2nd edn. RSC, London

Ponting, M. and Segal, I., 1998, Inductively Coupled Plasma atomic emission spectroscopy analyses of roman military copper-alloy artefacts from the excavations at Masada, Israel, Archaeometry, 40 (1), 109-122, DOI: 10.1111/j.1475-4754.1998.tb00827.x.

Panvini R., 1996, Storia e archeologia dell'antica Gela. Societa ed. Internaz. Torino, 5-121.

Vandeginste, B. G. M., Massart, D. L., Buydens, L. M. C., De Jong, S., Lewi, P. J. and Smeyers Verbeke, J., 1998, Handbook of Chemometrics and Qualimetrics Part B  1st Edition, in Data Handling in Science and Technology Volume 20B, Elsevier Science.

Zhengfeng, L., Yingdong, Y. and Wugan, L., 2016, A Lead Isotope Study of the Han Dynasty Bronze Artifacts from Liangshan Yi Autonomous Prefecture Museum, Sichuan Province, Southwest China, Current Analytical Chemistry, 12 (6), 553-559, DOI: 10.2174/1573411011666150901185450.